 CMES, vol.22, no.2, pp.91-96, 2007

A Comparative Study of Non-separable Wavelet and Tensor-product Wavelet in Image Compression

Jun Zhang[1]

Abstract: The most commonly used wavelets for image processing are the tensor-product of univariate wavelets, which have a disadvantage of giving a particular importance to the horizontal and vertical directions. In this paper, a new class of wavelet, non-separable wavelet, is investigated for image compression applications. The comparative results of image compression preprocessed with two different kinds of wavelet transform are presented: (1) non-separable wavelet transform; (2) tensor-product wavelet transform. The results of our experiments show that in the same vanishing moment, the non-separable wavelets perform better than the tensor-product wavelets in dealing with still images.

Keyword: Non-separable Wavelet; Tensor-product Wavelet; Image Compression

1 Introduction

Univariate wavelets have played an important role in signal processing since wavelet expansions became more appropriate than conventional Fourier series to characterize the local behavior of non-stationary signals [Antonini M, Barlaud M, and MathieuP, et al (1992), Mira Mitra, S. Gopalakrishnan (2006), Duddeck, Fabian M.E (2006)]. To apply wavelet methods to digital image processing, bivariate wavelets have to be constructed. The most commonly used method is the tensor product of univariate wavelets. This construction leads to a separable wavelet, which has a disadvantage of giving a particular importance to the horizontal and vertical directions [W. He and M. J. Lai (2000)]. There has been a growing research interest in the area of construction of non-separable wavelets over the past few years. Much effort has been made on constructing non-separable bivariate wavelet. For example, J.Kovacevic and Vetterli studied properties of multidimensional non-separable wavelets and numerically constructed examples of continuous non-separable compactly supported bivariate wavelets [J.Kovacevic and M.Vetterli (1992)]. Cohen and Daubechies generalized the method [I.Daubechies (1988)] to construct non-separable bidimensional (discontinuous) compactly supported wavelets [A. Cohen, I.Daubechies (1993)]. Both Cohen-Daubechies's wavelets and J.Kovacevic -Vetterli's examples are based on the dilation matrix $\left[\begin{smallmatrix}1 & 1\\ 1 & -1\end{smallmatrix}\right]$. Also, Ming-Jun Lai constructed bivariate non-separable compactly supported orthonormal wavelets based on the commonly used uniform dilation matrix $\left[\begin{smallmatrix}2 & 0\\ 0 & 2\end{smallmatrix}\right]$, which have 1-order vanishing moment and linear phase [W. He, M. J. Lai (2000)]. David stanhill and Yehoshua Y.Zeevi [D. Stanhill and Y.Zeevi (1996)] constructed the non-separable orthonormal wavelets based on the commonly used uniform dilation matrix $\left[\begin{smallmatrix}2 & 0\\ 0 & 2\end{smallmatrix}\right]$, which holds higher-order vanishing moment.

In this paper, four classes of non-separable wavelet filter banks with different properties are studied for image compression. The first one is Lai's non-separable wavelet based on the dilation $\left[\begin{smallmatrix}2 & 0\\ 0 & 2\end{smallmatrix}\right]$ that holds 1-order vanishing moment and linear phase. The second one is David stanhill's non-separable orthonormal wavelet based on the dilation $\left[\begin{smallmatrix}2 & 0\\ 0 & 2\end{smallmatrix}\right]$ that holds higher-order vanishing moment, but does no have the linear phase. The third one is the non-separable orthonormal wavelet based on the dilation $\left[\begin{smallmatrix}1 & 1\\ 1 & -1\end{smallmatrix}\right]$ that holds 1-order vanishing moment. The fourth one is the non-separable orthonormal wavelet based on

[1] Information Engineering College, Guangdong University of Technology, Guangzhou, 510006, China, e-mail: zhangjun7907@hotmail.com

the dilation $\begin{bmatrix} 1 & 1 \\ 1 & -1 \end{bmatrix}$ that holds higher-order vanishing moment. For the purpose of comparison, we also implemented the image compression method using tensor-product of univariate wavelets (CDF53, DB97).

2 Wavelet Transform in Two Dimensions: Non-separable Wavelet and Tensor Product of Univariate Wavelet

There are various ways to extend one-dimensional (1-D) wavelet transform to two dimensions. The simplest way to generate a 2-D wavelet transform is to apply two 1-D transforms separately. Thus, image decomposition can be computed with separable filtering along the abscissa and ordinate, by using the same pyramidal algorithm as in the 1-D case. As shown in Figure. 1, this separable transform (ST) called "tensor-product" decomposes images with a multi-resolution scale factor of two, providing one low-resolution subimage and three spatially oriented wavelet coefficient subimages at each resolution level.

Another way of extending wavelet transform to higher dimensions is to use non-separable filters. The 2-D MRA (multiresolution analysis) with a dilation matrix D is a ladder of closed subspaces $\{V_j\}_{j\in Z}$, which approximates $L^2(R^2)$ and satisfies

$$\{0\} \to \dots V_{-1} \subset V_0 \subset V_1 \dots \to L^2(R^2)$$

$$f(x) \subset V_{j-1} \Leftrightarrow f(Mx) \subset V_j \quad \exists \phi \in V_0 \text{s.t.}$$

Where, the set $\{\phi(x-k)\}_{k\in Z^2}$ is an orthonormal basis for V_0. The function $\phi(x)$ is called scaling function and since $V_0 \subset V_1$, $\phi(x)$ has to be the solution of a dilation equation of the form

$$\phi(x) = \sum_{k\in Z^2} H\phi(Dx-k)$$

The associated wavelet is then derived from the scaling function by the formula

$$\psi_i(x) = \sum_{k\in Z^2} G_i\phi(Dx-k) \quad i = 1,\dots,\det(D)-1$$

As shown in Figure. 2, the commonly transforms of non-separable wavelet are quincunx transform (QT) and separable sampling wavelets transform (FST) with four bands. The former bases on the dilation matrix $D = \begin{bmatrix} 1 & 1 \\ 1 & -1 \end{bmatrix}$, and the latter bases on the dilation $D = \begin{bmatrix} 2 & 0 \\ 0 & 2 \end{bmatrix}$ and uses non-separable and nonoriented filters ($M = \det(D)$).

3 The Image Compression Scheme

The standard process of image compression is as shown in Figure 3.

Where, Y denotes the wavelet coefficients that are obtained by performing wavelet transform to image data. A compression scheme can be designed as below [Wang Ling and Song Guo-xiang (2001)]:

1. Perform 8-bit Scalar quantization of Y
2. Let D_j^e denote the wavelet coefficients of part $e(e = H$ denotes horizontal; $e = V$ denotes vertical; $e = D$ denotes diagonal). δ_j^e denotes the threshold.
   $$D_{j,\delta}^e = \begin{cases} D_j^e, & \text{when abs}(D_j^e) > \delta_j^e \\ 0, & \text{otherwise} \end{cases}$$
3. Compute the entropy ofD_j^e, which is denoted ast_j^e.
   $$t_j^e = -\sum_k \sum_l p(D_{j,\delta}^e(k,l)) \log p(D_{j,\delta}^e(k,l))$$
   $p(D_{j,\delta}^e(k,l))$ is the probability of pixel (k,l) in $D_{j,\delta}^e$.

Compute the compression rate as following:

$$CR = 8 \Big/ \left\{ \frac{1}{\det(D)}(a_1t_1^H + a_2t_1^V + a_3t_1^D) + \dots + \frac{1}{(\det(D))^j}(a_1t_j^H + a_2t_j^V + a_3t_j^D) + \frac{1}{(\det(D))^j}t_j^L \right\}$$

a_1, a_2, a_3 all can set 1.

4 Experiment

In our experiment, the non-separable wavelet method is used to implement the image compression scheme. As a comparison, the tensor-product method of well-known biorthogonal wavelets CDF53 and DB97 (the best wavelet for image compression so far) is also implemented. The non-separable wavelet filter banks used in the experiments are as following:

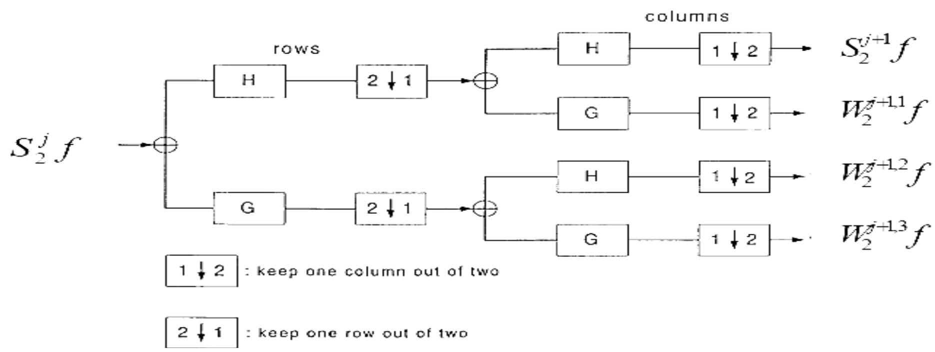

Figure 1: Tensor-product wavelet decomposition of $S_2^j f$

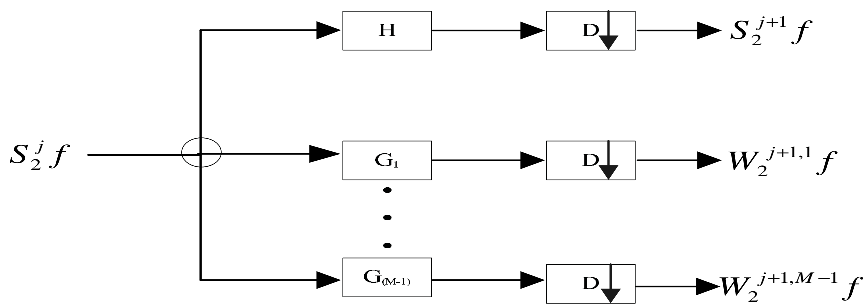

Figure 2: Non-separable wavelet decomposition of $S_2^j f$

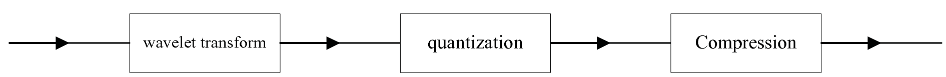

Figure 3: The processing of image compression

Quincunx Wavelet:

Orthogonal, 1-order vanishing moment (2-M1):

$$H = [\frac{1}{\sqrt{2}}, \frac{1}{\sqrt{2}}], \quad G = [\frac{1}{\sqrt{2}}, -\frac{1}{\sqrt{2}}]$$

Orthogonal, 2-order vanishing moment (2-M2):

$$H = \frac{1}{4 \times \sqrt{2}} \times \begin{bmatrix} 0 & 0 & 0 & 0 \\ 1+\sqrt{3} & 3+\sqrt{3} & 3-\sqrt{3} & 1-\sqrt{3} \\ 0 & 0 & 0 & 0 \end{bmatrix}$$

$$G = \frac{1}{4 \times \sqrt{2}} \times \begin{bmatrix} 0 & 0 & 0 & 0 \\ \sqrt{3}-1 & 3-\sqrt{3} & -3-\sqrt{3} & 1+\sqrt{3} \\ 0 & 0 & 0 & 0 \end{bmatrix}$$

Four-band, Separable Sampling Wavelet

Orthogonal, Linear phase, 1-order vanishing moment (4-M1):

$$H = \begin{bmatrix} 0.12438 & 0.124065 & 0.134125 & 0.134441 \\ 0.125309 & -0.124997 & -0.116181 & 0.134125 \\ 0.116492 & -0.13257 & -0.124997 & 0.124065 \\ 0.115563 & 0.116492 & 0.125309 & 0.12438 \end{bmatrix}$$

$$G_1 = \begin{bmatrix} 0.119815 & 0.103642 & -0.128752 & -0.129055 \\ 0.136266 & -0.120253 & 0.111526 & -0.128752 \\ 0.117017 & -0.143438 & 0.124518 & -0.114555 \\ 0.132964 & 0.142446 & -0.124211 & -0.114869 \\ 0.00393323 & -0.0044761 & -0.00422041 & 0.00418892 \\ 0.00390188 & 0.00393323 & 0.00423092 & 0.00419957 \end{bmatrix}$$

$$G_2 = \begin{bmatrix} G_{21} & G_{22} \end{bmatrix}$$

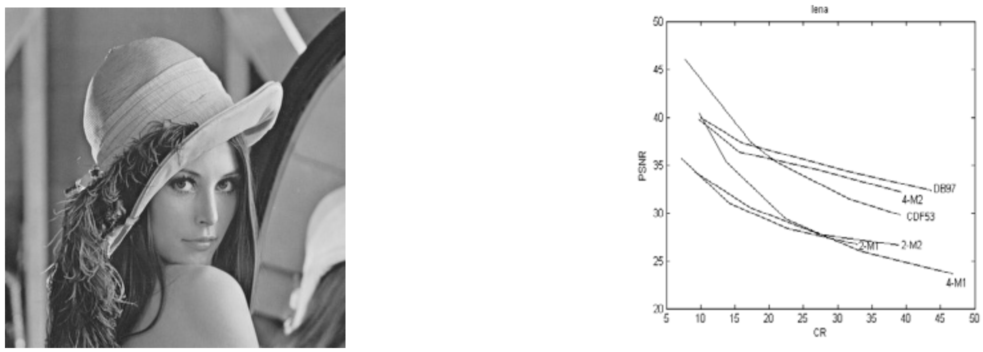

Figure 4: Lena

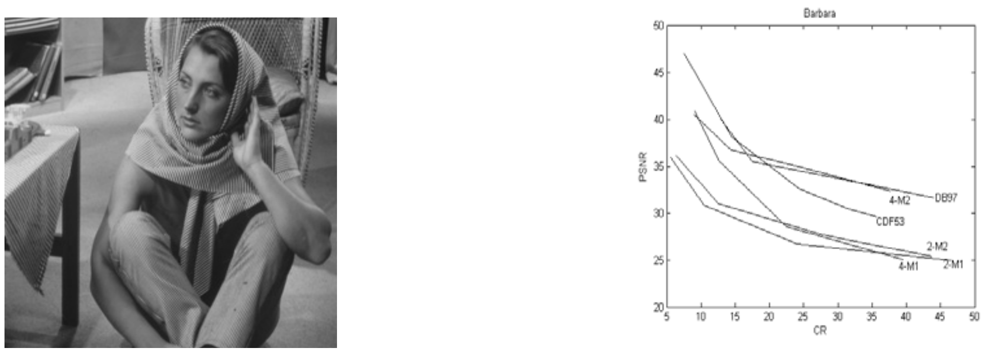

Figure 5: Barbara

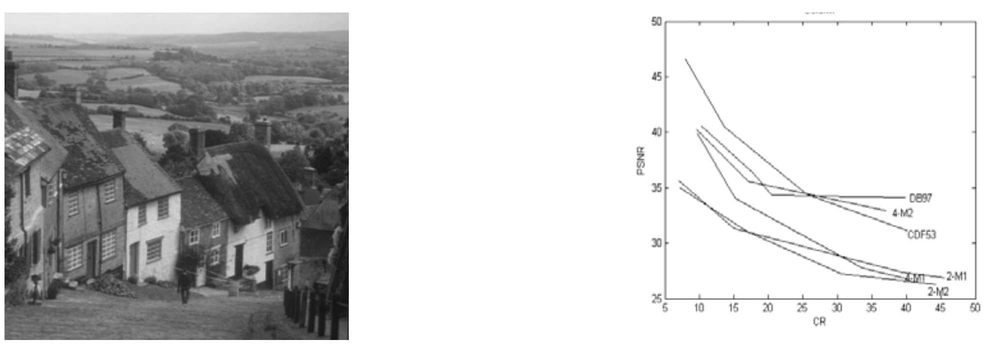

Figure 6: Barbara

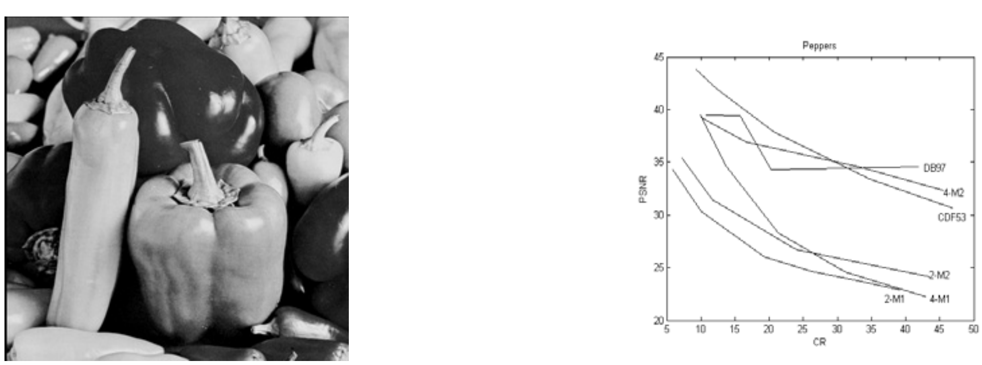

Figure 7: Pepper

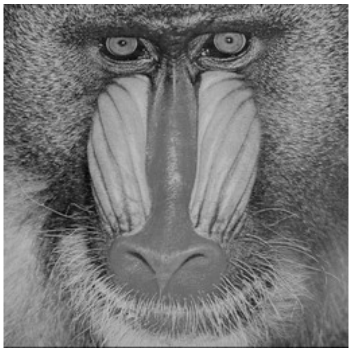

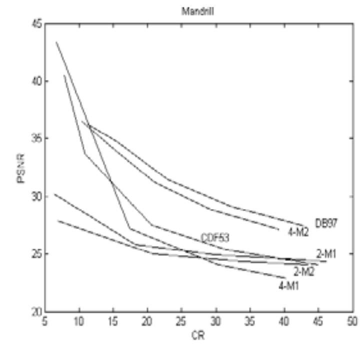

Figure 8: Mandrill

where

$$G_{21}=\begin{bmatrix}0 & 0 & 0.000127888\\ 0 & 0 & 0.000145448\\ 0.129237 & 0.111792 & 0.130945\\ 0.146981 & -0.129709 & -0.106902\\ -0.120619 & 0.137267 & 0.125783\\ -0.119657 & -0.120619 & -0.133362\end{bmatrix}$$

$$G_{22}=\begin{bmatrix}0.000110625 & -0.000137428 & -0.000137751\\ -0.000128356 & 0.000119041 & -0.000137428\\ 0.115243 & -0.00406622 & -0.00433127\\ 0.107394 & 0.00350473 & -0.00432173\\ -0.124314 & 0.00390884 & -0.00387968\\ -0.132429 & -0.00391858 & -0.00388954\end{bmatrix}$$

$$G_3=\begin{bmatrix}G_{31} & G_{32}\end{bmatrix}$$

where

$$G_{31}=\begin{bmatrix}0.124063 & 0.107316 & -0.137383\\ 0.141097 & -0.124516 & 0.110856\\ -0.111723 & 0.135288 & -0.12695\\ -0.110242 & -0.11987 & 0.134239\\ -0.0037948 & 0.00431857 & 0.00407185\\ -0.00376455 & -0.0037948 & -0.00408203\end{bmatrix}$$

$$G_{32}=\begin{bmatrix}-0.137147 & 0.00436924 & 0.00437951\\ -0.129236 & -0.00378467 & 0.00436924\\ 0.116734 & -0.00407191 & 0.00404148\\ 0.125177 & 0.00408205 & 0.00405175\\ -0.00404147 & 0 & 0\\ -0.00405178 & 0 & 0\end{bmatrix}$$

Orthogonal, 2-order vanishing moment (4-M2):

$$H=\frac{(3\times\sqrt{3}-1)}{416}\times \begin{bmatrix}9\sqrt{3}+16 & 9\sqrt{3}+16 & 4-\sqrt{3} & 4-\sqrt{3}\\ 16\sqrt{3}+27 & 16\sqrt{3}+27 & 4\sqrt{3}-3 & 4\sqrt{3}-3\\ 4-\sqrt{3} & 11\sqrt{3}+8 & 17\sqrt{3}-16 & 5\sqrt{3}-20\\ -8\sqrt{3}-7 & 4\sqrt{3}-3 & 12\sqrt{3}-9 & -13\end{bmatrix}$$

$$G_1=\frac{(1+\sqrt{3})}{8}\times\begin{bmatrix}2-\sqrt{3} & 2-\sqrt{3}\\ 2\sqrt{3}-3 & 2\sqrt{3}-3\\ -\sqrt{3} & -\sqrt{3}\\ 1 & 1\end{bmatrix}$$

$$G_3=\frac{1}{2}\times\begin{bmatrix}1 & -1\\ -1 & 1\end{bmatrix}$$

$$G_2=\frac{(5\times\sqrt{3}+7)}{416}\times \begin{bmatrix}4-\sqrt{3} & 4-\sqrt{3} & \sqrt{3}-4 & \sqrt{3}-4\\ 4\sqrt{3}-3 & 4\sqrt{3}-3 & 3-4\sqrt{3} & 3-4\sqrt{3}\\ 40-23\sqrt{3} & 45\sqrt{3}-76 & 16-17\sqrt{3} & 20-5\sqrt{3}\\ 47-28\sqrt{3} & 40\sqrt{3}-69 & 9-12\sqrt{3} & 13\end{bmatrix}$$

The peak signal to noise ratio (PSNR) for a gray-scale image $x$and its compressed reconstruction $\overline{x}$ is given by

$$RMSE=\sqrt{\frac{\sum\limits_{i\le M,j\le N}(x_{i,j}-\overline{x}_{i,j})^2}{NM}}$$

$$PSNR=20\log_{10}(\frac{255}{RMSE})$$

Because this application is image dependent, we have chosen five images: Lena, Barbara, Goldhill, Peppers and mandrill of size 256×256. The results are shown in Figure.4–Figure.8:

As shown in the Figure.4–Figure.8, DB97 has the best ascendant performance. Although the performance of the non-separable wavelet in these experiments is not as good as DB97, which is the best wavelet in image compression applications, the performance of the four-band, 2-order vanishing moment non-separable wavelet is close to that of DB97 and better than that of CDF53 that is also an excellent wavelet in image compression applications. Multidimensional non-separable wavelet is far away from being well understood so far. We believe that the non-separable wavelet will perform better and better in image compression applications as the advance of non-separable wavelet theory.

5 Conclusion

In this paper, we present the comparative results of image compression preprocessed with two different wavelet transforms: the non-separable wavelet transforms (quincunx and four-band) and the Tensor-product wavelet transform. The results show that: 1) the vanishing moment is an important property in still image compression 2) the four-band, 2-order vanishing moment non-separable wavelet has better performance in still image compression than Quincunx non-separable wavelet 3) the non-separable wavelet has better ascendant performance than the tensor-product of univariate wavelet. As the future work, we will investigate the application of non-separable wavelets in image compression.

References

Antonini, M.; Barlaud, M.; MathieuP et al. (1992): Image coding using wavelet transform. *IEEE Trans.Image Processing*, vol.1, pp.205-220.

Cohen, A.; Daubechies, I. (1993): Nonseparable dimensional wavelet bases. *Revista Mat. Iberoamericana*, Vol.9, pp.51-137.

Daubechies, I. (1988): Orthonormal bases of compactly supported wavelets. *Comm. Pure Appl.Math*, vol.41, pp.909-996.

Duddeck; Fabian, M.E. (2006): An alternative approach to boundary element methods via the Fourier transform. *CMES: Computer Modeling in Engineering & Sciences,* vol.16, pp.1-13.

He, W.; Lai, M.J.(2000): Examples of bivariate nonseparable compactly supported orthonormal continuous wavelets. *IEEE Trans. Image Processing*, vol.9, pp.949–953.

Mitra, M.; Gopalakrishnan, S. (2006): Wavelet Based 2-D Spectral Finite Element Formulation for Wave Propagation Analysis in Isotropic Plates. *CMES: Computer Modeling in Engineering & Sciences*, vol.15, pp.49-67.

Kovacevic, J.; Vetterli, M. (1992): Nonseparable multi- dimensional perfect reconstruction filter banks and wavelet bases for r^n. *IEEE Trans.Info.Theory*, vol.38, pp.533-555.

Stanhill, D.; Zeevi, Y. (1996): Two-Dimensional Orthogonal Wavelets with Vanishing Moments. *IEEE Trans. Signal Processing*, vol.10, pp.2579-2589.

Wang, L.; Song, G. (2001): The Pre-Processing of Multiwavelet and Its application in Image Compression. *Journal of Electron*, vol.10, pp.1418-1420.